

SMALL INVERTED-U LOOP ANTENNA FOR MIMO APPLICATIONS

S.-Y. Lin* and I.-H. Liu

Department of Electronics Engineering, Cheng Shiu University, Kaohsiung County 83347, Taiwan, R.O.C.

Abstract—This article presents a novel technique for isolation enhancement between two closely packed antennas. First, an inverted-U loop antenna (IULA) integrated into the top edge of a laptop panel is designed for 2.6-GHz LTE application. The mutual coupling between two designed IULA antennas has considerable effects by the placing positions of them. The results indicate the ground of the two IULA antennas placing against each other obtain the best isolation. At last, a three-element MIMO antenna was designed and measured. Although the gap between two adjacent antennas is only 1 mm, the experimental results show that the proposed two-element and three-element MIMO antennas achieve more than 20 dB isolation within the operating band. The important performances of antenna efficiency, envelope correlation, and channel capacity are also presented.

1. INTRODUCTION

The modern 4G wireless communication technologies, including Worldwide Interoperability for Microwave Access (WiMAX), Ultra Mobile Broadband (UMB), and Long Term Evolution (LTE), require wider frequency spectrum and faster transmission speed to access enormous data, speech, and images. Therefore, advancements of spectral utilization efficiency and channel capacity are important subjects for the development of wireless communication systems. To meet this demand, Multiple-input multiple-output (MIMO) technique that provides higher data throughput and longer propagation range becomes an optimal solution. A MIMO antenna uses two or more antennas operating at the same frequency bands, which increases

Received 29 August 2012, Accepted 22 October 2012, Scheduled 25 October 2012

* Corresponding author: Shun-Yun Lin (yun@csu.edu.tw).

channel capacity but suffers mutual interference. To reduce the co-channel interference and raise channel capacity, spatial division multiple access (SDMA) technique [1] is an effective method for an antenna array or a MIMO antenna.

The mutual coupling from closed antennas is mainly through two ways [2]: radiation emission (RE, through electromagnetic coupling) and conduction emission (CE, through a common conductor such as the ground plane). In the prior literatures, diversities of polarization [3–5], feeding mechanism [6] and antenna element [7, 8] are useful methods to reduce RE coupling. For a finite ground plane, a decoupling mechanism [9–12] is widely applied to resolve CE coupling. For closer coupled antenna elements, the neutralization technique is useful for achieving high isolation through a coupling element [13–15]. However, the location and structure of the coupling element need be carefully adjusted to achieve more than 20 dB isolation, which is usually acceptable for most practical applications [16]. Furthermore, this strategy may not be suitable for a system with more than two ports.

Currently, the increasing system capacity has led to very intensive research on multi-element MIMO antennas. For a four-port system, a stepped connection between antenna ground and system ground has been used to obstruct the CE coupling in our previous study [17]. Furthermore, dissimilar elements [7, 18] with similar radiation characteristics are used in compact communication terminals. In addition, the six-port MIMO antenna is notable, especially for laptop applications. For this, six patch elements wrapping around the top edge of the 14-inch laptop screen have been implemented [19]. A space of 10 mm from edge to edge was used, although only 14 dB isolation between neighbor elements was achieved. Moreover, a 3-D structure and additional feeding network are not easy to fabricate.

In this study, an inverted-U loop antenna (IULA) was designed in the beginning, which was integrated into a mini-laptop computer for 2.6-GHz LTE band application. Because of the folded structure of the U-shaped, the loop occupied dimension is clearly reduced. A capacitive-fed patch was used to compensate the degrading impedance bandwidth [20] causing by the folded structure. After the proposed IULA antenna is designed, four possible fabrications for MIMO application are presented and studied. The placement for two IULA antennas with their ground plane face to face shows the best isolation. Finally, a three-element MIMO antenna is proposed and measured. The results demonstrate that the proposed IULA antenna reaches more than 20 dB in isolation over the entire operation band for 1 mm space between antennas.

2. ANTENNA DESIGN

Figure 1(a) shows the configuration and photograph of the proposed inverted-U loop antenna (IULA) that integrated into the top edge of a laptop panel. The integrated position is a better location for receiving RF signals [21] and eliminating EM interference from the RF circuitry [22]. The distance s_1 between the IULA and left edge of the laptop panel is used to shift the resonance of the proposed design. The laptop panel, which is made of a copper plate with a thickness 1 mm and dimensions 220×170 ($L \times W$) mm^2 , acts as a system ground and is suitable as a supporting plate for the 10-inch LCD screen [20]. For actual implementation, the antenna can be mounted on the system ground by soldering or screws. In this experimental study, copper tape was used for the integration. To the proposed antenna, a driven strip, a feeding patch and an L-shaped antenna ground is printed on an FR4 substrate with a thickness of 0.8 mm and a relative permittivity of 4.4. Figure 1(b) shows the front view of the IULA, which consists of an inverted-U shape driven strip and an L-shaped ground plane. One end of the driven strip is connected to the antenna ground, and the other end (open end) has a gap of 0.5 mm to the antenna ground. The back view of the IULA shown in Figure 1(c) is a square patch with side length s_3 , which is placed under the strip and is aligned with the open end. The probe of a 50- Ω coaxial cable is connected to the square patch (point A) and the outer conductor is connected to the grounding point (point D) through a via hole. For this fabrication, a coupled-fed method is used to excite the antenna.

Antenna parameters should be considered for actual applications in a mini-laptop. First, the antenna height ($W_g = 2 \times 1.5 + g_1 + g_2 + 1$) is reduced as much as possible to fit in the limited space between LCD panel and outer cover. However, the spaces of g_1 and g_2 need to be large enough to reduce the coupling effect between strips and introduce good impedance matching between the driven strip and the coaxial cable. For the 2.6-GHz LTE operation, the occupied dimension of IULA is $30 \times 9 \text{ mm}^2$. Other parameters obtained from repeated theoretical study are shown in Table 1.

According to the characteristics of a rectangular loop [23], a half-wavelength loop has a wider beamwidth for the case of $\gamma = 0.5$ (γ is the ratio of side lengths without exciting source to another side) that is the most attractive ratio for the broad-band impedance characteristics. For the proposed antenna with parameters listed in Table 1, the driven strip is designed to provide a nearly half-wavelength resonant current path ($A \rightarrow B \rightarrow C \rightarrow D$; path length $\approx 2 \times (20.5 + 6) \text{ mm}$) at 2.6 GHz. However, the parameter $\gamma = 0.29$ ($\gamma = W_s/L_s = 6/20.5$) in

our case indicates that this prototype is not a good case for wideband operation. Furthermore, the double folded structure clearly reduces the antenna size, but at the expense of impedance matching between the feeding patch and driven strip. To improve the impedance matching and broaden the operating bandwidth, coupled-fed method and larger size of current-null [24] are applied in this design.

Figure 2(a) shows reflection coefficient S_{11} of the proposed IULA. The simulation and measurement were obtained from the commercial microwave simulation software Ansoft HFSS and from the network analyzer, respectively. From the results, the reactance of the 50- Ω coaxial cable with length of 200 mm causes a band shift. However, a similar resonance mechanism between the measurement and simulation

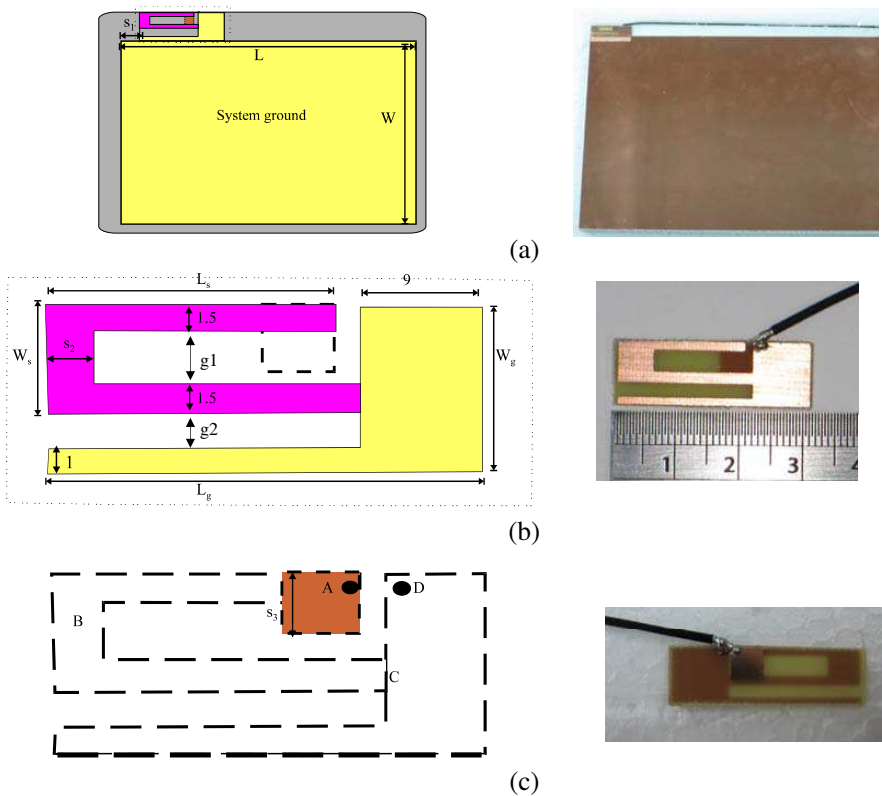


Figure 1. Configuration of the proposed IULA. In each sub-figure, the left and the right are schema and photograph, respectively. (a) The IULA integrated into a mini-laptop panel, (b) the front side and (c) the back side of the designed antenna.

Table 1. The antenna parameters of the proposed IULA shown in Figure 1. Unit of the physical size is mm.

L_s	W_s	g_1	g_2	L_g	W_g	s_1	s_2	s_3	L	W
20.5	6	3	2	30	9	0	5.5	5	220	170

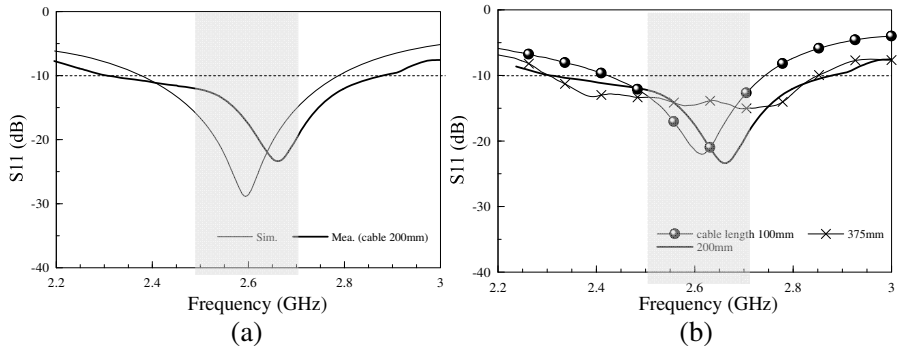


Figure 2. (a) Measured and simulated S_{11} of the proposed IULA. (b) Effects of cable length on measured S_{11} . Detailed antenna parameters are shown in Table 1.

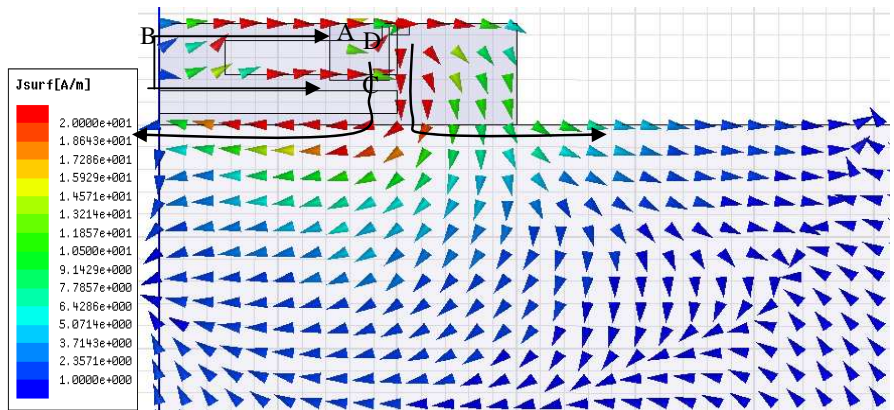


Figure 3. Simulated surface current distribution on the proposed IULA at resonance.

is seen. The measured impedance bandwidth based on $S_{11} \leq -10$ dB is from 2.314 to 2.876 GHz (21.0%). This bandwidth meets the requirement of 2.6-GHz LTE application band (2.500–2.690 GHz). The cable effect on the measurement S_{11} is shown in Figure 2(b) for cable lengths of 100 mm, 200 mm, and 375 mm. All the three cables are

parallel placed to the top edge of the system ground except the last case (375 mm) which has a left portion vertically bent along the vertical edge of the system ground. To compare the first two cases, the prototype with shorter cable has lower operating band and narrower bandwidth but more agrees with the simulation. On the other hand, the vertically bent cable causes different resonant mechanisms and disagrees with the simulation. According to the results, the cable with length of 200 mm is used to feed the IULA in this study. The surface current distribution, as shown in Figure 3, indicates that a half-wavelength resonance is successfully excited. The current on the driven strip is from current null (point B) respectively toward point A and point C, and is conducted left along the horizontal portion of antenna ground. Also, the system ground plane around the antenna ground has induced current caused by conduction.

Effects of the antenna's location/orientation, current-null dimen-

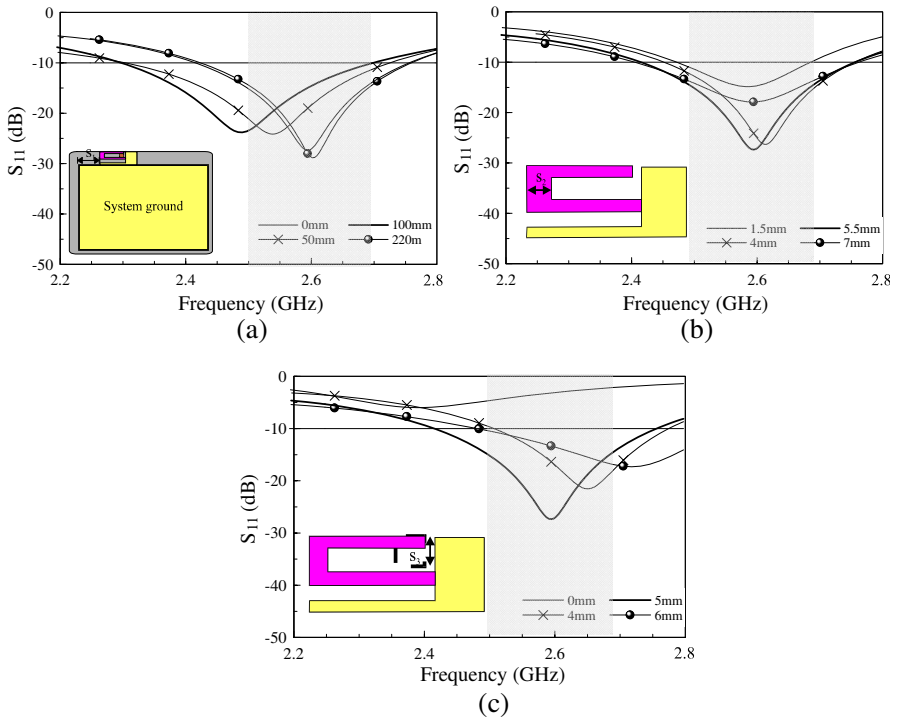


Figure 4. Simulated S_{11} in frequency of the proposed antenna against (a) s_1 , (b) s_2 , and (c) s_3 . The original parameters are the same as Table 1.

sion, and feeding patch on S_{11} are theoretically presented in Figure 4. When the driven strip is on left of the antenna ground, we refer to this fabrication as a left orientation, whereas the right orientation is opposite. In Figure 4(a), varied s_1 represents the different location of antenna on the top edge of system ground. Especially, the case of $s_1 = 220$ mm indicates that the antenna is in right orientation and located at the upper-right corner. The simulation results indicate that the frequency response of the proposed antenna is practically independent of antenna orientation. However, because the current path on the system ground is lengthened as the antenna is located away from the upper-left corner of system ground (increased s_1), the operating band shifts toward lower frequency. Figure 4(b) shows different lengths of s_2 , which enlarges the current-null size as s_2 is increased. The simulated results show that the bandwidth is broadened from 8.3% ($s_2 = 1.5$ mm) to 14.2% ($s_2 = 7$ mm). In Figure 4(c), the inductive input impedance mismatches the 50- Ω source impedance as directive feed ($s_3 = 0$) is considered. For the cases of $s_3 = 4, 5,$ and 6 mm, capacitive feeds compensate inductive input impedance to obtain impedance matching in interested band.


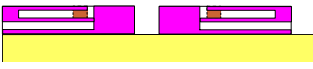


3. IULA IN MIMO APPLICATION FOR MINI-LAPTOP

3.1. Two IULA Elements in a Laptop Terminal

This section performs and studies two IULA elements for two-port MIMO antenna designs. The possible fabrications for MIMO can be divided into four designs as shown in Table 2. In each design, the two IULA elements are marked #1 (element 1) and #2 (element 2). The gap (d) between the two elements is set as 1 mm in this study. Design 4 is not considered because the neighboring vertical strips, which have null current and strong electrical field, will cause strong coupling and poor isolation between the elements.

Figure 5 shows the simulated surface currents in vectors on the inverted U-strips and the ground planes of Designs 1, 2, and 3. To explain the effect of field cancellation between the elements, element 1 is excited, while element 2 is terminated by a 50- Ω load in the simulation. The induced current on the inactive element 2 has two parts, which are from radiation-emission (RE) coupling and from conduction-emission (CE) coupling. For example, the Design 1 shown in Figure 5(a), the antenna ground of element 1 is next to the vertical strip of element 2 and causes an EM-coupling. The induced current (bold line \rightarrow dot line; RE-induced current) on the strip of element 2 is in phase along the loop. This is a common exciting path for conventional half-wavelength loop. On the other hand, the CE-

Table 2. The possible fabrications of two-port MIMO antenna with IULA elements.

Design 1	
Design 2	
Design 3	
Design 4	

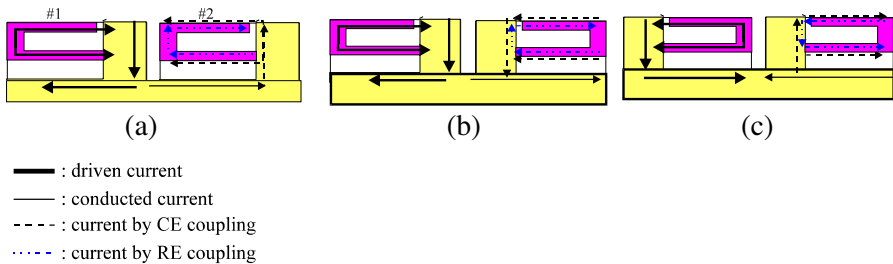


Figure 5. Simulated surface current in vector on antenna elements and ground plane at resonance for (a) Design 1, (b) Design 2, and (c) Design 3.

induced current, which is conducted from one integrated conductor (system ground and antenna ground) to the strip of element 2, has similar distribution as the driven strip of element 1. It can be seen that the currents on the upper portion of driven strip are in opposite directions. Although this feature introduces a partial field cancellation, the isolation between two closely packed antenna elements is still enhanced. The other prototypes can be deduced by analogy.

For experimental studies, isolation coefficient S_{ij} is the same as S_{ji} for a passive circuitry. In addition, the reflection coefficient S_{ii} of the i th element is active when other elements are terminated by a $50\text{-}\Omega$ load. For the original parameter shown in Table 1, Figures 6(a), (b), and (c) respectively show the S -parameters of Designs 1, 2 and 3. A

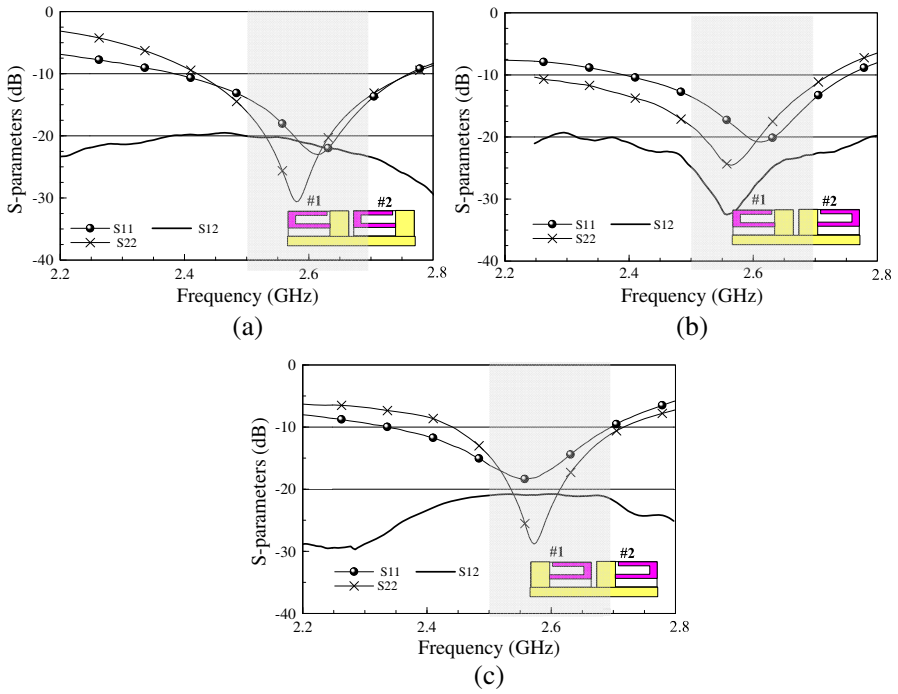


Figure 6. Measured S_{11} , S_{22} , and S_{12} of the proposed two-port MIMO antenna. (a) Design 1, (b) Design 2, and (c) Design 3.

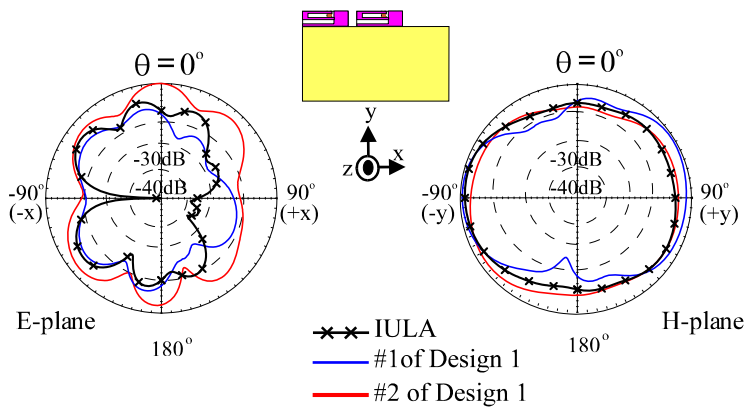


Figure 7. Measured far-field radiation patterns of the proposed IULA, and antenna elements of Design 1.

cable-feed for antenna exciting is expected for laptop terminals. Due to the outer conductor shielding, the interference between the cables and the cable effect on isolation between antenna elements should be very little. In that case, the simulation results should agree with the measurement. The experimental results show that the operating bands of all antenna elements are shifted toward lower frequencies except for element 1 of Design 2. This is caused by the lengthened current path on the system ground. However, the 10-dB impedance bandwidths of all antenna elements still meet the requirement of the 2.6-GHz LTE band. Moreover, isolations between antenna elements of all studied prototypes are less than 20 dB within the 2.6-GHz LTE band although the space between the elements is only 1 mm. Particularly in Design 2, the shielding effect caused by the antenna ground enhances the highest isolation between the elements.

The far-field radiation patterns of Designs 1, 2 and 3 were measured in an anechoic chamber. All the proposed prototypes have similar radiation patterns. Here, the measured results of Design 1 are presented. For clear comparison, the proposed IULA (shown in Figure 1) is also presented. Figure 7 plots the measured radiation patterns in the E - and H -planes at the central frequency of 2.6-GHz LTE band. The measured radiation patterns are similar to that of the rectangular loop antenna [23]. In addition, the similarities between IULA and MIMO antenna indicate the advanced isolation of the proposed IULA in MIMO antenna system. Figure 8 presents the measured peak antenna gain against frequency. The gain variation of each case is less than 1 dB and the gain differences between elements are less than 3 dB. These characteristics indicate that IULA is a promising candidate for a multi-port MIMO antenna system.

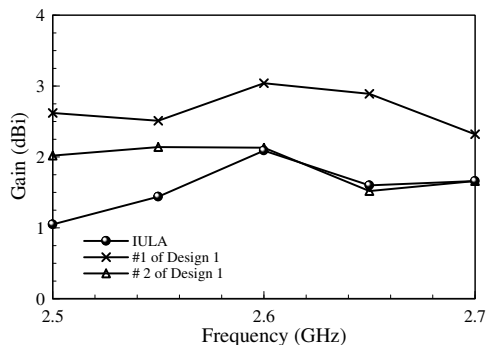


Figure 8. Measured peak antenna gain against frequency of the proposed IULA, element 1 and element 2 of Design 1.

3.2. Multi-port IULA MIMO Antenna in a Laptop Terminal

A three-element arrangement based on Design 1 or Design 3 described in part A is implemented. Although Design 2 has a better isolation, the prototype is not suitable for the MIMO antenna system with more than 2 ports. In Figure 9(a), a three-port IULA MIMO antenna has been integrated on the upper-left edge of the system ground with a uniform spacing of 1 mm. The overall dimensions are $92 \times 9 \times 0.8 \text{ mm}^3$. For further application, another module of three-port MIMO antenna (indicated in dotted line) can be symmetrically integrated on the upper-right edge of the system ground to carry out a six-port MIMO antenna. The space (about 16 mm) between the two modules is suitable to embed a CCD camera. Owing to the limited measurement capacity of our laboratory, only a three-port MIMO antenna was investigated. In our previous study [25], the L-shaped antenna ground preserves the original performances from a CCD camera. Therefore, the embedded CCD camera was not considered in experimental measurement. Figure 9(b) shows a photograph of the proposed three-port MIMO antenna.

Figure 10 (a) shows the measured reflection coefficient of each I/O port. Owing to the different current path of each port (discussed in Figure 4(a)), the center frequency of the three operating bands has small shifts. Fortunately, the 10-dB impedance bandwidth of each port still meets the application band of 2.6 GHz-LTE.) Figure 10(b) shows the isolation among the three ports. The measured isolations between adjacent ports (S_{12} and S_{23}) are better than 20 dB within the operating band and the nonadjacent port (S_{13}) reaches 25 dB because of further distance between them.

To examine the performances of the proposed MIMO antennas, the important factors of antenna efficiency, envelope correlation, and

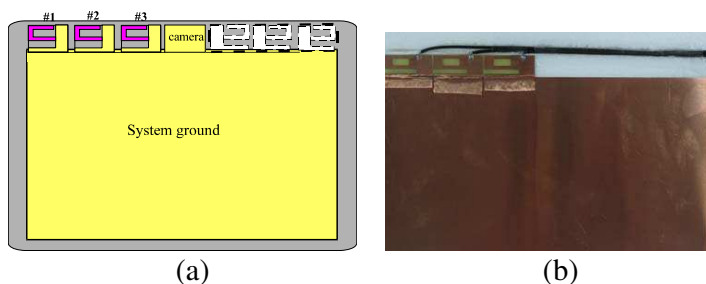


Figure 9. (a) Configuration of the proposed three-port MIMO antenna and possible prototype of six-port MIMO antenna in a laptop panel. (b) Photograph of the of the proposed three-port MIMO antenna.

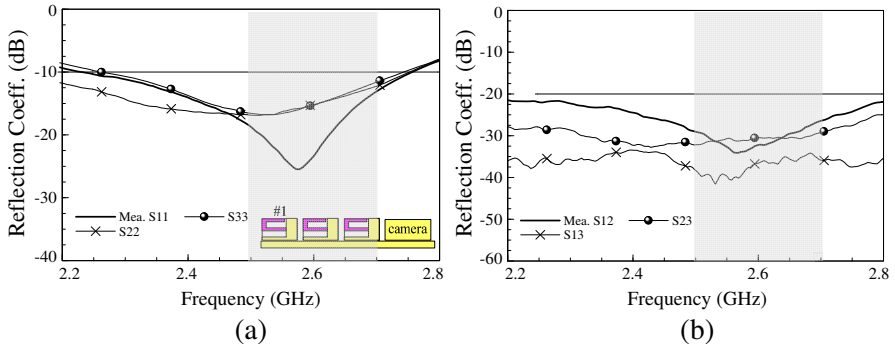


Figure 10. Measured S -parameters of the proposed three-port MIMO antenna. (a) Reflection Coeff. S_{11} , S_{22} , and S_{33} . (b) Isolation Coeff. S_{12} , S_{23} , and S_{13} .

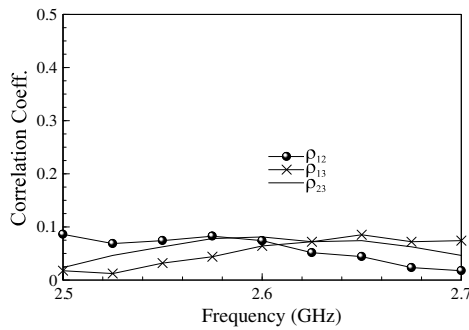


Figure 11. Measured Correlation coefficients of the proposed three-port MIMO antenna.

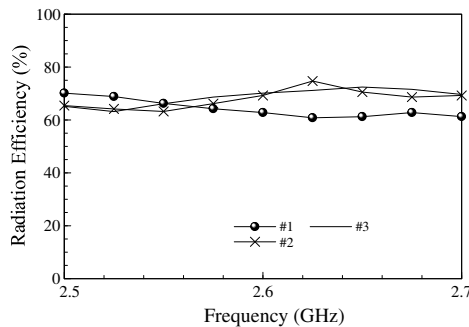


Figure 12. Measured radiation efficiencies of each antenna elements of the proposed three-port MIMO antenna.

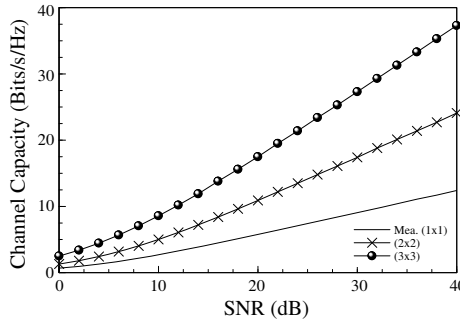


Figure 13. Measured channel capacities for 1×1 , 2×2 , and 3×3 MIMO antenna systems of the proposed three-port MIMO antenna.

channel capacity were measured through the Bluetest HP700 [26]. The reverberation chamber is a metal cavity with dimension of $1.2 \times 1.75 \times 1.8 \text{ m}^3$, which is large enough to support several cavity modes for the operation over $650 \sim 6000 \text{ MHz}$. The modes can be stirred to create a Rayleigh distributed transfer function between a fixed wall mounted antenna (Tx) and the antenna under test (Rx) inside the chamber. In the measurement scheme, we place three printed monopoles at the transmitter and experimentally study our proposed three-port IULA MIMO antenna. The isolation between all three monopoles is greater than 20 dB and we consider that they will provide uncorrelated Tx signals.

Figure 11 plots the measured correlation coefficients of ρ_{12} , ρ_{13} and ρ_{23} . These coefficients are all less than 0.1 within the interested bandwidth, which demonstrate another good performance of this design [27]. Radiation efficiency is also an important parameter for an antenna applying in a multipath propagation environment. The measured radiation efficiencies of the three elements plotted in Figure 12 are varied within $65\% \sim 75\%$, which are reasonable comparing to the conventional printed antenna with a loopy substrate [28].

When we measure the three-element IULA array in the reverberation chamber with three fixed wall antennas (as in our case), we can define $3 \times 3 = 9$ channels, and find the combined capacity of the 9 channels from the channel matrix $\mathbf{H}_{3 \times 3\text{-MIMO}}$ formed by the normalized transmission coefficient S_{21} . The instantaneous maximum capacity of the MIMO system takes the known form:

$$C_{3 \times 3\text{-MIMO}} = \log_2 \left(\det \left(\mathbf{I}_M + \frac{SNR}{3} \mathbf{H}\mathbf{H}^* \right) \right);$$

\mathbf{H} is the channel matrix $\mathbf{H}_{3 \times 3\text{-MIMO}}$. We use all the measured

samples of the 3×3 channel matrix $\mathbf{H}_{3 \times 3\text{-MIMO}}$ to calculate the mean capacity $C_{3 \times 3\text{-MIMO}}$ as a function of the SNR by averaging all values of the instantaneous capacity. More detail explanations of the channel capacity measurement can be found from Ref. [26]. The measured channel capacities for 1×1 , 2×2 , and 3×3 MIMO antenna systems at the band of 2.6 GHz-LTE are shown in Figure 13. At 20 dB SNR the channel capacities are 5.7, 10.9, and 17.5 b/s/Hz for single IULA, two-port, and three-port MIMO antenna, respectively. The channel capacity is proportionally increased with the increasing port number.

4. CONCLUSIONS

The designed IULA prototype on top edge of a mini-laptop panel has been successfully constructed integrated and tested. Experimental and measuring studies confirmed that the operating bandwidth and performances are suitable for 2.6-GHz LTE application. The prototype incorporates two and three IULA elements forming the multi-element antenna for MIMO system on a laptop terminal. Although the gap for adjacent elements has only 1 mm, the antenna isolations for two-port and three-port are all better than 20 dB. The stable and good radiation efficiency and linearly increasing channel capacity also demonstrate the reliability of the design. Furthermore, the compact and small dimensions indicate that the proposed antennas are well suitable for internal MIMO antennas of a wireless mini-laptop.

REFERENCES

1. Liberti, J. C. and T. S. Rappaport, *Smart Antennas for Wireless Communication Communications: IS-95 and Third Generation CDMA Applications*, Prentice Hall PTR, 1999.
2. Paul, C. R., *Introduction to Electromagnetic Compatibility*, Wiley, 1992.
3. Wong, K. L., H. C. Tung, and T. W. Chiou, "Broadband dual-polarized aperture-coupled patch antennas with modified H-shaped coupling slots," *IEEE Trans. on Antennas and Propaga.*, Vol. 50, 188–191, 2002.
4. Lin, S. Y. and K. C. Huang, "A compact microstrip antenna for GPS and DCS application," *IEEE Trans. on Antennas and Propaga.*, Vol. 53, 1227–1229, 2005.
5. Su, S. W., "High-gain dual-loop antennas for MIMO access points in the 2.4/5.2/5.8 GHz bands," *IEEE Trans. on Antenna and Propaga.*, Vol. 58, 2412–2419, 2010.

6. Wong, H., K. L. Lau, and K. M. Luk, "Design of dual-polarized L-probe patch antenna arrays with high isolation," *IEEE Trans. on Antenna and Propaga.*, Vol. 52, 45–52, 2004.
7. Li, H., J. Xiong, and S. He, "A compact planar MIMO antenna system of four elements with similar radiation characteristics and isolation structure," *IEEE Antennas and Wireless Propaga. Lett.*, Vol. 8, 1107–1110, 2009.
8. Delaveaud, C. and C. Brocheton, "Compact combined antenna with dual dipolar-type radiation," *Microwave Opt. Technol. Lett.*, Vol. 38, 415–418, 2003.
9. Krairiksh, M., P. Keowsawat, C. Phongcharoenpanich, and S. Kosulvit, "Two-probe excited circular ring antenna for MIMO application," *Progress In Electromagnetics Research*, Vol. 97, 417–431, 2009.
10. Chiu, C. Y., C. H. Cheng, R. D. Murch, and C. R. Rowell, "Reduction of mutual coupling between closely-packed antenna elements," *IEEE Trans. on Antenna and Propaga.*, Vol. 55, 1732–1738, 2007.
11. Li, J. F., Q. X. Chu, and X. X. Guo, "Tri-band four-element MIMO antenna with high isolation," *Progress In Electromagnetics Research C*, Vol. 24, 235–249, 2011.
12. Chen, S. C., Y. S. Wang, and S. J. Chung, "A decoupling technique for increasing the port isolation between two strongly coupled antennas," *IEEE Trans. on Antenna and Propaga.*, Vol. 56, 3650–3658, 2008.
13. Mak, A. C. K., C. R. Rowell, and R. D. Murch, "Isolation enhancement between two closely packed antennas," *IEEE Trans. on Antenna and Propaga.*, Vol. 56, 3411–3419, 2008.
14. Diallo, A., C. Luxey, P. L. Thuc, R. Staraj, and G. Kossiavas, "Study and reduction of the mutual coupling between two mobile phone PIFAs operating in the DCS1800 and UMTS bands antennas and propagation," *IEEE Trans. on Antenna and Propaga.*, Vol. 54, 3063–3074, 2006.
15. Kim, Y., J. Itoh, and H. Morishita, "Decoupling method between two L-shaped folded monopole antennas for handsets using a bridge line," *IET Microwaves, Antennas and Propaga.*, Vol. 4, 863–870, 2010.
16. Wong, K.-L., J.-H. Chou, C.-L. Tang, and S.-H. Yeh, "Integrated internal GSM/DCS and WLAN antennas with optimized isolation for a PDA phone," *Microwave Opt. Technol. Lett.*, Vol. 46, 323–326, 2005.

17. Lin, S. Y. and H. R. Huang, "Ultra-wideband MIMO antenna with enhanced isolation," *Microwave Opt. Technol. Lett.*, Vol. 51, 570–573, 2009.
18. Chiu, C. Y. and R. D. Murch, "Compact four-port antenna suitable for portable MIMO devices," *IEEE Antennas and Wireless Propaga. Lett.*, Vol. 7, 142–144, 2008.
19. Guterman, J., A. A. Moreira, and C. Peixeiro, "Integration of omnidirectional wrapped microstrip antennas into laptops," *IEEE Antennas and Wireless Propaga. Lett.*, Vol. 5, 141–144, 2006.
20. Lin, Y. C., S. Y. Lin, H. W. Wu, and W. S. Cheng, "A $\lambda/2$ loop antenna for GPS application in mini-laptop," *Asia Pacific Microwave Conference*, 1852–1855, 2009.
21. Bernhard, J. T., "Analysis of integrated antenna positions on a laptop computer for mobile data communication," *IEEE Symp. on Antennas and Propag.*, 2210–2213, 1997,.
22. Huff, G. H., J. Feng, S. Zhang, G. Cung, and J. T. Bernhard, "Directional reconfigurable antennas on laptop computers: Simulation, measurement and evaluation of candidate integration positions," *IEEE Trans. on Antenna and Propaga.*, Vol. 52, 3220–3227, 2004.
23. Tsukiji, T. and S. Tou, "On polygonal loop antennas," *IEEE Trans. on Antenna and Propaga.*, Vol. 28, 571–575, 1980.
24. Chang, C.-H. and K.-L. Wong, "Internal coupled-fed shorted monopole antenna for GSM850/900/1800/1900/UMTS operation in the laptop computer," *IEEE Trans. on Antenna and Propaga.*, Vol. 56, 3600–3604, 2008.
25. Lin, S. Y., C. W. Guan, S. A. Yeh, and H. R. Huang, "EMC monopole antenna integrated with an L-shaped ground for handset application," *IEEE Antennas Propagat. Soc. Int. Symp. Dig.*, Jun. 2007.
26. Kildal, P.-S. and K. Rosengren, "Correlation and capacity of MIMO systems and mutual coupling, radiation efficiency, and diversity gain of their antennas: Simulations and measurements in a reverberation chamber," *IEEE Comm. Magazine*, 104–112, 2004.
27. Ko, S. C. K. and R. D. Murch, "Compact integrated diversity antenna for wireless communications," *IEEE Trans. on Antenna and Propaga.*, Vol. 49, 954–960, 2001.
28. Wong, K. L., *Compact and Broadband Microstrip Antennas*, Wiley, New York, 2002.